S. Dash
M. L. Joshi

Silicon Defect Structure Induced by Arsenic Diffusion and Subsequent Steam Oxidation

Abstract: Misfit dislocation nets are known to occur when very high amounts of phosphorus and boron are diffused into silicon single-crystal wafers. Diffusion of arsenic in silicon is not known to produce such dislocations. Through transmission electron microscopy it is shown in this paper that diffusion of high amounts (up to 1.6×10^{21} atoms/cm^3) of arsenic creates Frank hexagonal loops on (111) planes parallel to the diffusion surface, and stacking faults on the inclined {111} planes, instead of misfit dislocation nets (the latter are still not observed). These faults and loops are found to be extrinsic, and are thought to be due to insertion of extra silicon layers in the matrix where the stacking fault energy is decreased by arsenic atoms. The driving force for the generation of loops and faults is shown to be the concentration gradient rather than fast cooling.

Introduction

Solute concentration gradients imposed by diffusion of large amounts of phosphorus and boron have been known to cause generation of misfit dislocation networks and also precipitates in highly perfect single crystal silicon wafers.[1-4] Diffusion of arsenic, however, has not yet been observed to cause such dislocations.[3]

The amount of solute concentration in the impurity-diffused surfaces necessary to develop stresses sufficient to cause plastic deformation will depend primarily upon the size of the impurity atom in the host lattice of silicon, i.e., upon the misfit ratio of the diffusing atoms. This misfit ratio is defined as the ratio

$$\frac{\Delta r}{r} = \frac{r_{Si} - r_I}{r_{Si}},$$

where r_{Si} and r_I are the tetrahedral covalent radii of the silicon and the impurity atom. Using Pauling's data[5] on the tetrahedral covalent radii, we find that the misfit ratios $\Delta r/r \approx 0.25$, 0.066 and 0.008 for B, P and As respectively. On this basis, the surface concentration of arsenic needed to develop stresses sufficient to cause plastic deformation within layers immediate to the surface is expected to be considerably higher than the surface concentrations of boron and phosphorus.

The term "surface concentration" should be defined unambiguously. It is known that the actual surface concentration C_{ST}, measured with the radio-tracer techniques, the surface concentration C_{SE}, obtained electrically by careful measurement of the diffusion profile, and the surface concentration C_S, determined from the surface resistivity and the junction depth assuming the hypothetical erfc distribution, differ widely from each other. To avoid confusion, we will use C_S values (unless otherwise mentioned) to indicate the surface concentration, since these are the values most widely used in the semiconductor industry and literature. With this point in mind, let us estimate the arsenic surface concentration needed for dislocation generation using the Prussin[1] model of generation and distribution of dislocations by solute diffusion.

The maximum stress developed at the beginning of the diffusion process owing to the lattice contraction caused by the solute is given by[1]

$$\sigma_x(\max) = \beta C_S E/(1 - \nu), \qquad (1)$$

where

β = solute lattice contraction coefficient
= $n(\Delta r/r)/C_S$, n being the solute fraction,
C_S = surface concentration,
E = Young's modulus, and
ν = Poisson's ratio.

The surface concentration of B, P and As needed to exceed the yield stress ($\approx 7 \times 10^8$ dynes/cm^2 at 1150°C) in silicon then can be deduced from Equation (1). It is found that $C_S(B):C_S(P):C_S(As) :: 1:4:20$. Dislocation generation through diffusion is known to start from sur-

S. Dash is with the Fairchild Semiconductor Research and Development Laboratory, Palo Alto, California 94304; M. L. Joshi is located at the IBM Components Division Laboratory in Burlington, Vermont 05452.

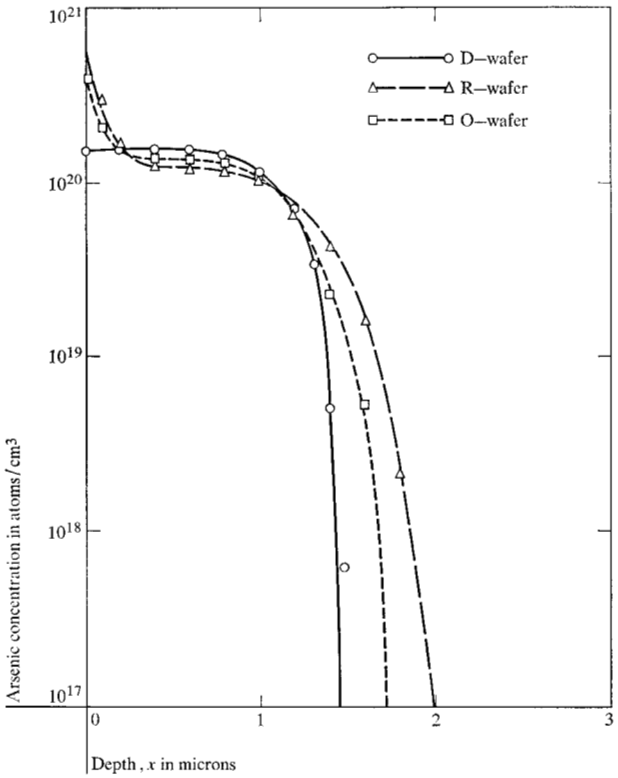

Figure 1 Arsenic diffusion profiles for D-, O- and R-wafers. Note the increase in arsenic concentration near the surface in O- and R-wafers.

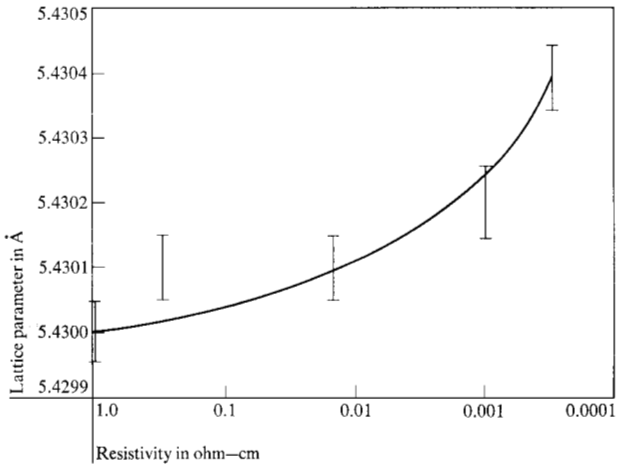

Figure 2 Lattice parameter of silicon as a function of arsenic concentration in silicon powder.

face concentrations as small as 10^{20} atoms/cm^3 of boron and 3×10^{20} atoms/cm^3 of phosphorus. This observation is in agreement with the simple criterion given above. The same criterion gives C_S for arsenic to be $\approx 2 \times 10^{21}$ atoms/cm^3. Such a high surface concentration of arsenic has not yet been reported to have been achieved through diffusion and, consequently, it is not surprising that misfit dislocations have not yet been observed through arsenic diffusion.

Recently it has become possible to achieve a C_S for arsenic as high as 1.6×10^{21} atoms/cm^3. In samples of silicon diffused with arsenic to that concentration, no misfit dislocation nets could be observed. Instead, prismatic dislocation loops and stacking faults were seen. These defects have been observed through transmission electron microscopy, and their crystallographic nature has been investigated through diffraction contrast techniques. The results of these investigations and an interpretation of the whole phenomenon are presented.

Experimental

• *Diffusion*

Arsenic was diffused in an evacuated closed quartz capsule (vacuum $\approx 10^{-8}$ torr) into high resistivity p-type clean and damage free single-crystal silicon wafers at 1200°C for 90 minutes, using a powder of a master alloy of silicon and arsenic made by the usual freeze-out method. The diffusion step described above is usually referred to as "deposition" and therefore we will henceforth refer to these wafers as D-wafers. The surface concentration of arsenic in the D-wafers was found to be 1.7×10^{21} atoms/cm^3.

In order to enhance C_S in the D-wafers, some of them were steam oxidized at 1200°C until an oxide of about 5000 Å thickness (30 minutes) was obtained. These wafers, henceforth, will be called O-wafers. Some of the O-wafers were reoxidized using the same treatment as above; these wafers will be called R-wafers. The oxidation treatment[6] helped increase the surface concentration of arsenic in the wafers.

Some of the p-type wafers were steam oxidized in the "pure" state, because it is known that silicon crystals of p type often contain large amounts of nonequilibrium oxygen. A steam oxidation treatment can precipitate this oxygen and also induce stacking faults.[7] The process was found, however, to cause no such effects in our samples.

Diffusion profiles of D-, O- and R-wafers were obtained electrically with a four point probe; these profiles are shown in Fig. 1. It should be understood that since the profiles do not represent erfc distributions, the surface concentrations C_S initially determined are quite different from the C_S values in Fig. 1. The tendency of the oxidation steps, however, to enhance the surface concentration is obvious from this figure.

• *X-ray lattice parameter measurements*

Silicon crystals grown with various amounts of arsenic doping, corresponding to resistivities 1, 0.3, 0.015, 0.001 and 0.0003 ohm-cm, were powdered and precise lattice

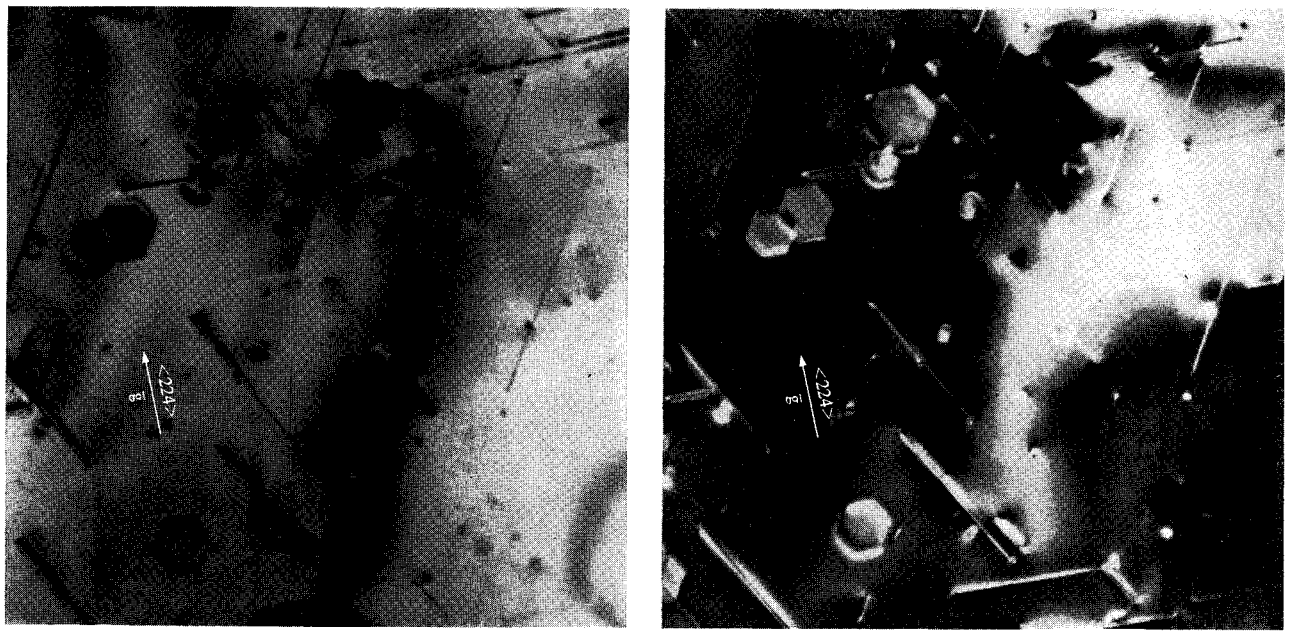

Figure 3 Sessile Frank loops in O-wafers parallel to the (111) foil surface and stacking faults parallel to the inclined {111} planes. (a) and (b) Bright and dark fields with a prominent ⟨224⟩ diffusion vector.

parameters were determined. The lattice parameter curve for various arsenic concentrations is shown in Fig. 2. (It should be borne in mind here that these lattice parameter values are only relative, not absolute.) The maximum lattice parameter a_0 (for the 0.0003 ohm-cm resistivity sample) is 5.4304 Å for an impurity concentration of 3×10^{20} atoms/cm^3. Since the actual surface concentration of arsenic in the R-wafers is about 10^{21} atoms/cm^3 (i.e., resistivity <0.0001 ohm-cm), a much larger lattice parameter is expected to result in the R-wafer surface. A possible extrapolated value of a_0 for 0.0001 ohm-cm resistivity material is $\approx 5.4305 \pm 0.00005$ Å. This implies that the diffusion of arsenic caused a 10^{-4} (approximately) fractional lattice expansion in the R-wafers.

• *Electron transmission microscopy*

The oxide on the samples was removed by HF acid. Very small samples were then cut from the larger ones to fit the sample holder of the electron microscope. These small samples were chemically thinned to make the surface of interest transparent to the electron beam; this surface was protected by a resistant wax and the thinning was done from the opposite side of the sample. This method of thinning usually leaves a hole at the center of the sample, but the thin portion (3000 to 8000 Å thick) around the hole provides a region large enough for the electron-microscopic observations.

In general, three types of diffusion-induced defects were observed:

1) Frank loops[8] of hexagonal type and lying parallel to the (111) surface of the silicon wafers;
2) stacking faults lying on the inclined {111} planes of the silicon wafers;
3) dislocation networks.

The geometrical nature of the dislocation loops and stacking faults was examined in O-wafers using diffraction contrast techniques. The dislocation networks were observed mostly in R-wafers. It has to be pointed out that the size of the hexagonal loops and also the length of the stacking faults increased with increasing periods of diffusion anneal. This was evidenced by the observation that the hexagonal loops and the stacking faults in R-wafers were significantly larger than those in O-wafers. This suggests that the cooling rate of the wafers was not responsible for the increase. The driving force is not supersaturation as a result of the fast cooling, but rather a concentration gradient of the impurity.

The dislocation loops are generated in the surface layers (diffusion surfaces), and they stay near the surface because they are sessile. Further, when a layer of about 200 Å was removed by anodic oxidation and subsequent dissolution by hydrofluoric acid, the small dislocation loops vanished. The detailed results are presented below.

Frank loops

Figures 3(a) and (b) show a general area of the O-wafers in bright and dark fields for the reflection vector g as

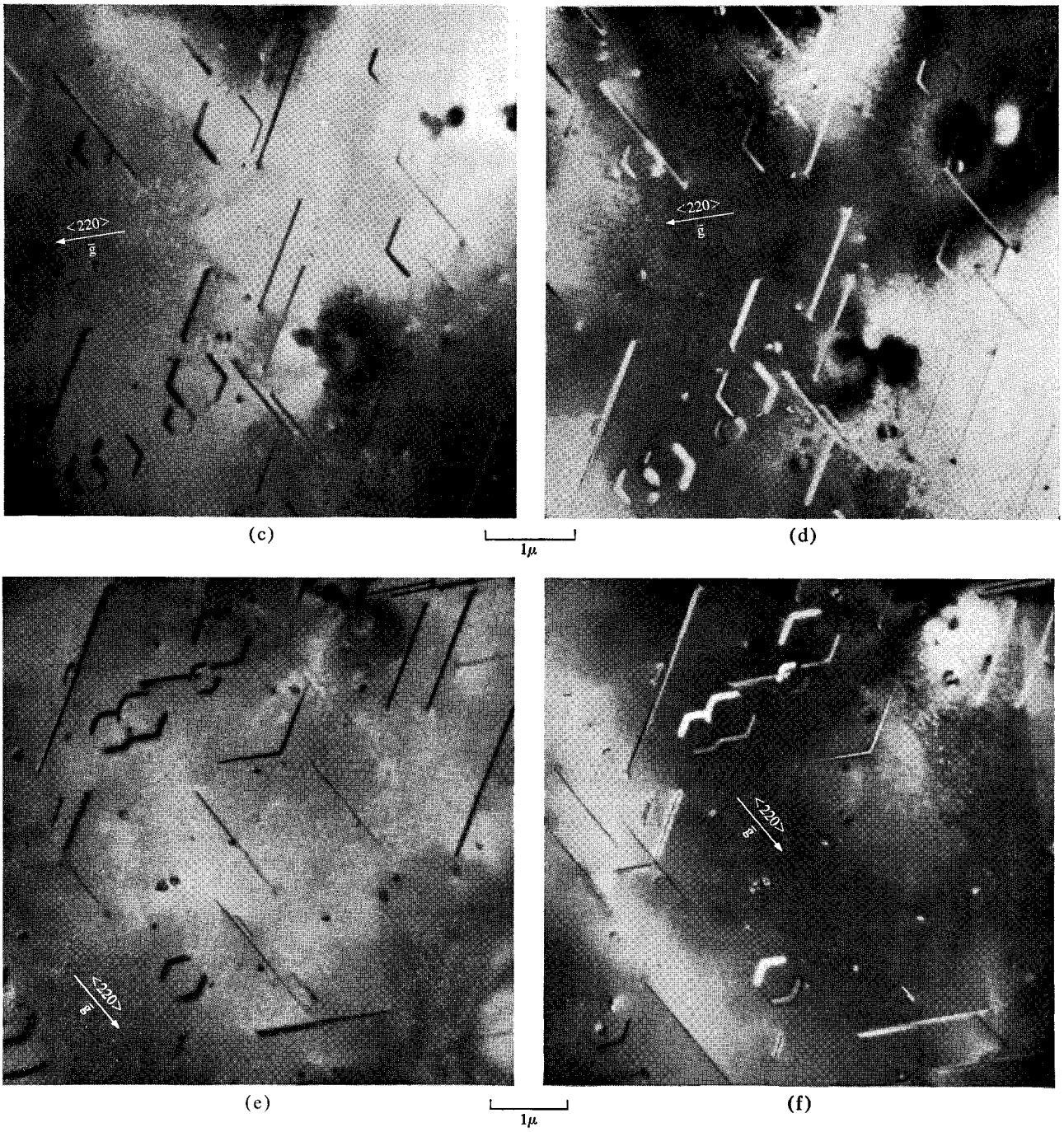

Figure 3 (c) and (d) Bright and dark fields of the same view as in Fig. 3 (a) with a prominent ⟨220⟩ diffraction vector; (e) and (f) bright and dark fields of the same view as in (a) with a second prominent ⟨220⟩ reflection vector.

shown. One can observe the dislocation loops of different sizes and the stacking faults in the same region. The dislocation loops and stacking faults are distributed evenly throughout the domain of observation. Figure 4 shows a histogram for the distribution of the dislocation loops with the sizes (2 × edge length) of the loops in O- and R-wafers. It was found that the loops of size smaller than 600 Å were too numerous and too small to be resolved and measured. With the highest magnification, the smallest discernible hexagonal loop was about 150 Å. The largest hexagonal loop was about 18,000 Å. In Figs. 3(a) and (b) for $\mathbf{g} = \langle 224 \rangle$, we observe a uniform "residual contrast" inside the loops. Although other reflections are present, they are operating only weakly. The only domi-

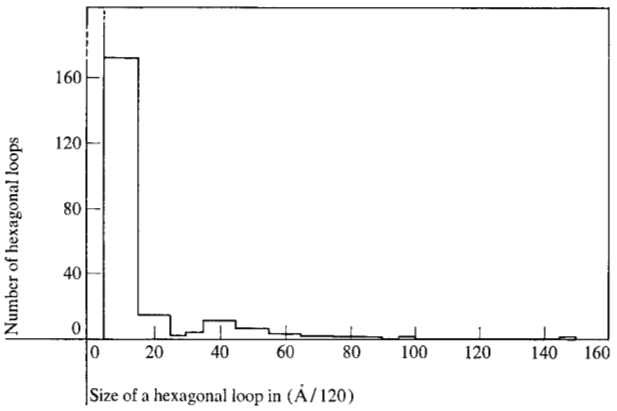

Figure 4 Frequency of occurrence of Frank loops in O- and R-wafers as a function of their size. The smallest observed loop diameter is 150 Å. A number on the abscissa scale should be multiplied by the number 120 to find the size of a loop.

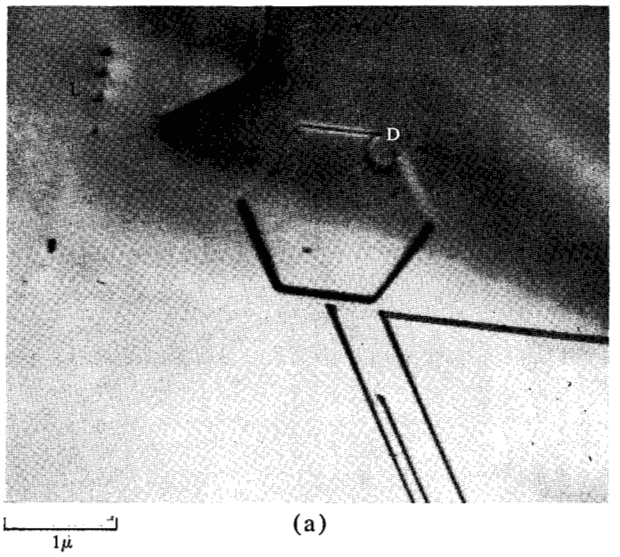

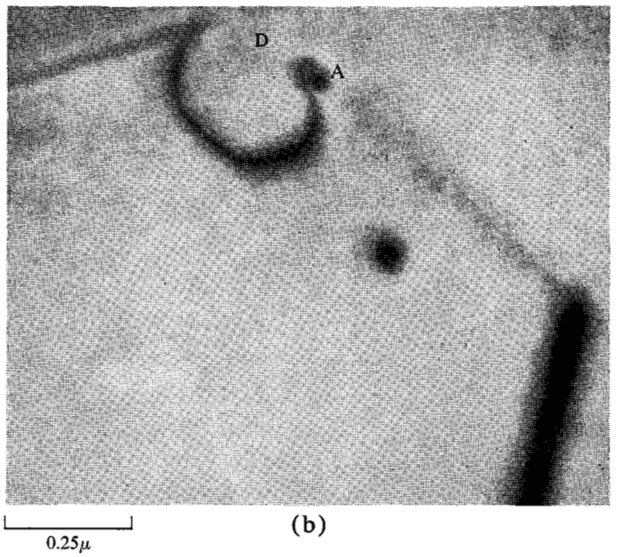

Figure 5 (a) The largest Frank loop observed in the process of unfaulting; (b) magnified image of the Frank loop in (a). Note the climb of the dislocation at the anchor point A.

nant reflection corresponds to $\langle 224 \rangle$; consequently one should conclude that these loops contain stacking faults.[9]

The same set of hexagonal loops upon tilting showed for a pure two-beam case that edges parallel to the **g** (true for all the three possible $\langle 220 \rangle$) vanished. This is exemplified in Figs. 3(c) through 3(f). From these contrast experiments one observes that the loops obey the contrast predictions for **b** perpendicular to the foil plane, i.e., $\mathbf{g} \cdot \mathbf{b} \times \mathbf{u}$ contrast, with $\mathbf{g} \cdot \mathbf{b} = 0$.[10] The Burgers vector is most probably $\frac{1}{3}a \langle 111 \rangle$.

Some of the very small dislocation loops [e.g., P in Fig. 6(a)] causing black and white contrast were analyzed. It was mentioned earlier that these loops were within 200 Å of the diffusion surface (also the top surface of the film). Since the extinction distance for $\mathbf{g} = \langle 220 \rangle$ in silicon[10] is 757 Å, it is felt that the loops were almost at the surface. Hence, they were interstitial in nature.[11] We cannot be sure, however, that this is so since the depth measurement is subject to significant error. It will be shown later that the nature of the stacking faults is a better criterion for judging the nature of the Frank loops.

Figures 5(a) and (b) show the process of disappearance of a hexagonal loop by "climb." This was very rarely observed. Figure 5(b) is just the magnified image of the loop in Fig. 5(a) and this loop is seen at D in the process of unfaulting.

Stacking faults

Extensive faulting was observed in O-wafers. However, the stacking fault density was considerably higher in R-wafers. Stacking faults were found in large numbers in the regions where Frank loops were observed. The length of the faults varied widely. The preponderance of stacking faults indicates that arsenic lowers the stacking fault energy of silicon. In the bright field view of Fig. 6(a) at B and C, stacking faults are observed to interact. The image of a single stacking fault was always found to be trapezoidal in shape and the longer parallel side was determined to be the top side of the foil, i.e., the surface where the diffusion begins. The method for determining topside is illustrated in Fig. 6(b). If the position of the topside is known, then so is the sense of inclination of the plane containing the fault.

Very small faults bounded by a dislocation on all sides at E and F, i.e., small dislocation loops containing faults, are observed in Fig. 6(a). As these loops grow in size, they are intersected by the wafer surface. Some of the

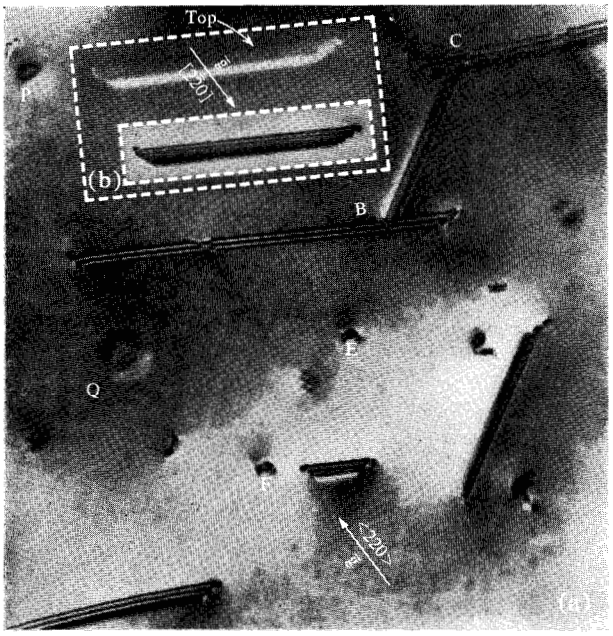

Figure 6 (a) Note the extremely small Frank loops E, F, etc., lying on inclined {111} planes, and the extremely small Frank hexagonal loop P lying parallel to the (111) foil surface and intersecting the stacking faults on inclined {111} planes; (b) illustration of extrinsic nature of stacking fault.

larger faults observed in Fig. 6(a) and all the other figures clearly showing stacking fault fringes are the result of this process. The bounded loops on inclined ⟨111⟩ are Frank loops of the type found on the foil plane. Therefore, the nature of the stacking faults is most probably the same as that of the Frank loops. One cannot be sure of this, however, since the nature of the bounding partial of the inclined stacking fault is not determined. The single stacking faults [like the ones in Figs. 6(a) and (b)] were analyzed and found to be extrinsic.[9] In this connection, it must be mentioned that the analysis of Art et al.[9] applies to foils where thickness is greater than four times the extinction distance (i.e., to thick foils). The faults analyzed in this experiment were indeed in the thick region, as shown in Fig. 6(b), where the depth is about five times the extinction distance. Therefore the Frank loops on the foil plane also enclose an extrinsic fault; i.e., they are interstitial loops.

The observation that the inclined stacking faults were predominantly larger than those parallel to the foil plane needs explanation.* Only dislocations with a large component of the Burgers vector lying in the foil plane are expected to relieve misfit stresses, but only Frank loops with a Burgers vector of $\frac{1}{3}\langle 111\rangle$ inclined to the foil plane may also help relieve misfit stresses. This may account for the larger size of the inclined loops.

Dislocation tangles

Dislocation tangles occur due to the growth of sessile loops and the interaction among them in R-wafers. (A detailed account of this phenomenon is planned for future publication.) Misfit dislocation nets, however, were not observed in any of the samples. This is understandable since, as explained above, arsenic does not introduce more than a 10^{-4} fractional lattice expansion in the diffusion zone, even for values of C_S as high as 10^{21} atoms/cm^3.

Discussion

The major result of the diffusion of high concentrations of arsenic is the generation of hexagonal extrinsic Frank loops of sessile type on {111} planes. Hexagonal loops of such type have been obtained by Dash[12] and Phillips and Dash[13] by diffusion of gold at temperatures about 1000°C. Dash interpreted the hexagonal loops to be extra planes of silicon atoms and not platelets of gold coherent with the silicon lattice. The present observations are exactly similar to those of Dash, and therefore it is not necessary to assume the loops to be arsenic platelets coherent with the silicon lattice. The existence of a few arsenic atoms in association with the loops, however, cannot be ruled out.

Although splitting of a dislocation is difficult in covalently bonded crystals, it has been shown by researchers that the stacking fault energy in silicon is only ≈40 ergs/cm^2 for the intrinsic type and ≈60 ergs/cm^2 for the extrinsic type. Consequently a Frank edge loop with $\frac{1}{3}\langle 111\rangle$ as a Burgers vector is expected to be more stable than a prismatic loop with a perfect Burgers vector, $\frac{1}{2}\langle 110\rangle$. The generation of Frank loops in preference to the prismatic loops in silicon diffused with arsenic is consistent with these considerations. Stability of a Frank loop is, however, not possible at all sizes, and beyond a certain critical size the prismatic loops are expected to be stable. In Fig. 4 we have plotted a statistical size distribution for the Frank loops observed in O- and R-wafers. It should be informative, in the light of such data, to estimate and compare the stability range of the Frank loops and the prismatic loops. The energy[14] of a Frank hexagonal loop can be shown to be

$$E_{FH} = \frac{\gamma L^2\sqrt{6}}{4} + \frac{\mu a^2 L}{2\pi(1-\nu)\sqrt{6}} \ln\left(\frac{2L}{a\sqrt{3}}\right). \qquad (2)$$

The energy[15] of a prismatic hexagonal loop also can be proved to be

$$E_{PH} = \frac{3\mu a^2 L}{4\pi(1-\nu)\sqrt{6}} \ln\left(\frac{2L}{a\sqrt{6}}\right), \qquad (3)$$

* Due to E. Levine; see Acknowledgments.

where

a = lattice parameter,
γ = extrinsic stacking fault energy
= 60 ergs/cm^2 (as a rough estimate[15]),
L = length of a side of a hexagon,
μ = shear modulus = 7.55×10^{11} dynes/cm^2, and
ν = Poisson's ratio = 0.27.

It was found (using these equations) that the Frank hexagonal loops have lower configuration energy for edge lengths up to 3000 Å. Most of the observed hexagonal loops do possess edge lengths of less than 3000 Å. It is very likely that the stacking fault energy of silicon is reduced by the presence of arsenic atoms and consequently some Frank loops of edge lengths larger than 3000 Å are stable. We have seen in Fig. 5 that the largest observed Frank loop is in the process of unfaulting through nucleation of another loop at one of its corners (D). This is equivalent to rejection of interstitials or absorption of vacancies for an extrinsic fault.

The smallest observed dislocation loops were approximately 150 Å in diameter. The critical size at which an interstitial cluster in the form of a disc collapses into a Frank loop* can be easily estimated using the criterion for small loops,

$$E_D + E_\gamma - E_S = 0\,, \tag{5}$$

where

$E_D = 2\pi r_c \mu b^2$ = energy of dislocation loop of radius r_c and Burgers vector b,
$E_\gamma = \pi r_c^2 \gamma$ = stacking fault energy,
and $E_S = A\gamma_S$ = surface energy of a disc having total surface area A.

We will use the value $\gamma_S = 1250$ ergs/cm^2 and the previous values for the other parameters. With the approximations that the loop area, $\pi r_c^2 \approx (\sqrt{3}/4)a^2 I$ (I being the number of interstitials associated with the loop) and also that $A \approx (\sqrt{3}/2)Ia^2$, it is found that the critical diameter of a Frank loop is about 120 Å, which is not far from the smallest observed size of 150 Å. The number of interstitials associated with such a loop is $\approx$720. The largest stable loop was calculated before to be $\approx$3000 Å in edge length. The number of interstitials associated with such a loop is $\approx 3 \times 10^5$.

By counting the number of loops and their individual sizes in an electron micrograph, it is possible to estimate the interstitial density generated. The film thickness, of course, should be known. From Fig. 3(a) for the particular situation the concentration of interstitials is estimated to be $\approx 10^{16}$ per cm^3 with the knowledge that the film is about 3000 Å in depth from the surface as previously indicated. This concentration is considerably greater than the vacancy equilibrium concentration in intrinsic silicon at the diffusion temperature.[16] Creation of such a large number of interstitials during diffusion is shown next to be a possible result of the undersaturation of vacancies inside the dislocation-free silicon single crystals.

Supersaturation and condensation of interstitials of silicon cannot be ascribed to the possible rapid cooling of the surface layers of the arsenic-diffused wafers since the size of the hexagons was found to increase with increasing period of heat treatment, i.e., with the length of diffusion anneal time at a given oxidation temperature. Also, the silicon wafers are in a closed capsule and are thick. Cooling of the capsule in air is not likely to induce quenching effects. The gold-diffusion-induced Frank loops in the experiments by Dash[12] follow the same pattern. It is concluded by Dash that the rapid in-diffusion of interstitial gold results in the annihilation of most of the thermal vacancies present throughout the dislocation free silicon crystals and therefore the concentration of substitutional gold depends upon the supply of vacancies in the crystal. Since the diffusion of vacancies from the surface is a slow process (the energies of motion for vacancies and interstitials are 1.1 and 0.51eV, respectively, according to Benneman[17]) in comparison with the flow of interstitials, the silicon lattice tends to drive silicon or gold atoms from substitutional sites to interstitial sites in order to counteract the vacancy undersaturation. The interstitials created in this dissociative diffusion process cause the generation of Frank loops.

The analogy of the mechanism of Frank loops induced by gold is, however, not fully applicable to those induced by arsenic. Gold diffuses interstitially and occupies substitutional sites. Arsenic and all the other elements in columns III and V of the periodic table are known to diffuse mostly by a vacancy mechanism. In recent years, however, considerable evidence has been accumulated for the existence of a small interstitial diffusion component for these elements in Ge and Si.[18,19] Consequently, we can assume here a double stream diffusion for arsenic. Most of the arsenic atoms, however, occupy substitutional sites. When the arsenic concentration in the surface is higher than a certain amount, one could expect an interstitial flow of arsenic that would be sufficient to cause undersaturation of vacancies inside the crystal. Such an undersaturation can be relieved by the jumping of substitutional arsenic and silicon atoms into interstitial sites. The resulting interstitials could condense into Frank loops. Undersaturation of Schottky defects in a sodium chloride crystal[20] is known to produce prismatic dislocation loops. These two examples are indicative of an equilibrium in dislocation-free crystals created by the generation of dislocations during a chemical reaction in

* Here we have assumed that interstitials form clusters in localized areas, and that these clusters collapse to form loops in the same manner that vacancy voids collapse to give rise to vacancy loops.

which part of the released chemical energy is converted into the elastic energy of a system of dislocations.

As noted earlier, high-resistivity p-type silicon crystals, after steam oxidation following a certain high-temperature treatment,[7] exhibit precipitates of Si_xO_y complexes and extrinsic stacking faults if the oxygen content of the crystals is higher than the equilibrium value. Although when subjected to steam oxidation alone our silicon samples did not exhibit Frank loops nor extrinsic faults, it is possible that the presence of oxygen in association with high amounts of arsenic diffusant may be responsible for the observed defect structure. Of this, however, we are not certain.

Acknowledgments

We express gratitude to J. S. Makris who did the x-ray work. Sincere thanks are due to A. Platt who brought to the authors' attention the crystallographic problems associated with the diffusion of high concentrations of arsenic in silicon. The explanation for the size of inclined stacking faults was suggested[21] by Dr. E. Levine of the Department of Mechanics and Materials Science, Rutgers, whose advice in review of this paper is gratefully acknowledged.

References

1. S. Prussin, *J. Appl. Phys.* **32,** 1876 (1961).
2. J. Washburn, G. Thomas and H. J. Queisser, *J. Appl. Phys.* **35,** 1909 (1964).
3. M. L. Joshi and F. Wilhelm, *J. Electrochem. Soc.* **112,** 185 (1965).
4. M. L. Joshi and S. Dash, *IBM J. Res. Develop.* **11,** 271 (1967).
5. L. Pauling, *Nature of the Chemical Bond,* 3rd edn., Cornell University Press, New York 1960, p. 24.
6. A. S. Grove, O. Leistiko, Jr., and C. T. Sah, *J. Appl. Phys.* **35,** 2695 (1966).
7. M. L. Joshi, *Acta Metallurgica* **14,** 1157 (1966).
8. J. Friedel, *Dislocations,* Addison-Wesley Publishing Co. Inc., Reading, Mass. 1964, pp. 144–146.
9. A. Art, R. Gevers, and S. Amelinckx, *Phys. Stat. Sol.* **3,** 697 (1963).
10. P. B. Hirsch, A. Howie, R. B. Nicholsen, D. W. Pashley and M. J. Whelan, *Electron Microscopy of Thin Crystals,* Butterworths, Washington 1965, pp. 179, 341.
11. K. G. McIntyre, *Phil. Mag* **15,** 205 (1967).
12. W. C. Dash, *J. Appl. Phys.* **31,** 2275 (1960).
13. V. A. Phillips and W. C. Dash, *J. Appl. Phys.* **33,** 568 (1962).
14. R. M. J. Cotterill, *Lattice Defects in Quenched Metals,* Academic Press, New York 1965, p. 143.
15. E. Aerts, P. Delavignette, R. Siems and S. Amelinckx, *J. Appl. Phys.* **33,** 3078 (1962).
16. M. L. Joshi, *J. Electrochem. Soc.* **112,** 912 (1965).
17. K. H. Benneman, *Phys. Rev.* **137A,** 1497 (1965).
18. V. E. Kosenko, *Sov. Phys.—Solid State* **3,** 1526 (1962).
19. S. Maekawa, *J. Phys. Soc. Japan* **17,** 1592 (1962).
20. A. S. Barber, K. H. Harvey and J. W. Mitchell, *Phil. Mag.* **2,** 704 (1957).
21. E. Levine, private communication.

Received February 7, 1968